Symmetry breaking in honeycomb photonic lattices

Omri Bahat-Treidel, Or Peleg, and Mordechai Segev*

Department of Physics and Solid State Institute, Technion-Israel Institute of Technology, Haifa 32000, Israel
**Corresponding author: msegev@tx.technion.ac.il*

Received July 24, 2008; revised August 25, 2008; accepted August 26, 2008;
posted September 4, 2008 (Doc. ID 99318); published September 30, 2008

We study the phenomena associated with symmetry breaking in honeycomb photonic lattices. As the honeycomb structure is gradually deformed, conical diffraction around its diabolic points becomes elliptic and eventually no longer occurs. As the deformation is further increased, a gap opens between the first two bands, and the lattice can support a gap soliton. The existence of the gap soliton serves as a means to detect the symmetry breaking and provide an estimate of the size of the gap. © 2008 Optical Society of America

OCIS codes: 190.2055, 190.6135.

Honeycomb lattices are intriguing systems, possessing a unique band structure [1,2]. Unlike other periodic systems, the first and second bands of honeycomb lattices do not overlap, yet they are not completely separated either. Instead, the first two bands intersect at a set of points, the diabolic points, irrespective of the depth of the potential of the individual lattice sites. The slope of the propagation constant surface at the vicinity of these points is linear. Hence the phase velocity is constant, and the effective mass in those regions is infinite. Recent advances in solid-state physics have attracted much interest in graphene, a carbon 2D honeycomb lattice where charge carriers with momentum corresponding to the diabolic points act as massless fermions obeying the Dirac equation. Hence these points are also called Dirac points, and electron states near them present unique features such as chiral tunneling [3] and room-temperature integer quantum Hall effect [4]. In another domain, matter–wave physics, honeycomb optical lattices give rise to excitations behaving like Dirac fermions [5]. Finally, recent work on honeycomb photonic lattices showed a band structure similar to that of graphene and also that a beam propagating in the direction associated with a Dirac point experiences conical diffraction [6]. That observation was the first evidence that conical diffraction is a more general phenomenon than occurring just in biaxial optical crystals [7–9].

Here, we study the dynamics of optical beams in a honeycomb photonic lattice whose symmetry is gradually deformed. We find that, when the honeycomb symmetry is complete, the conical diffraction pattern contains two bright rings separated by a dark ring, rather than a single bright ring as initially thought [6]. When the lattice is gradually deformed, the conical diffraction pattern becomes elliptic until, at some strong enough deformation, the diabolic points merge, then completely disappear, and a gap forms between the first and second bands. We show that the gap in such a strongly deformed lattice can be detected using a gap soliton: the existence of the soliton gives direct indication of the presence of a gap, providing an estimation on the size of the gap.

The paraxial propagation equation for a monochromatic wave ψ in a 2D photonic lattice is

$$i\frac{\partial\psi}{\partial z}+\frac{1}{2k}\nabla_{\perp}^{2}\psi+\frac{k\Delta n(|\psi|^{2})}{n_{0}}\psi=0, \tag{1}$$

where Δn is the modulation in the refractive index, k is the wavenumber in the medium, and n_0 the background refractive index. As demonstrated in [6], a honeycomb photonic lattice is readily generated by the optical induction technique, by transforming an intensity pattern I_{ind} into variations in the refractive index [10–12], using defocusing nonlinearity of the form $\Delta n=\Delta n_0/(1+I_{\mathrm{ind}}+B|\psi|^2)$ [13]. Here, Δn_0 is the maximal index change, I_{ind} and B are in units of the background illumination, and $\int|\psi(x,y)|^2\mathrm{d}x\mathrm{d}y=1$. Here, I_{ind} is formed by the interference of three plane waves as

$$I_{\mathrm{ind}}=\left|\sum_{i=1,2,3}\eta_i\exp[ik_0(x\cos\theta_i+y\sin\theta_i)]\right|^2, \tag{2}$$

where $k_0=(k_x^2+k_y^2)^{1/2}$ is the transverse wavenumber and $\theta_i=0,2\pi/3,4\pi/3$. We can choose $\eta_1=1$ and consider only the relative amplitudes η_2,η_3. When $\eta_2=\eta_3=1$, I_{ind} is a triangular pattern translated into a perfect honeycomb photonic lattice of lattice constant $D=4\pi/(3k_0)$, as shown in Fig. 1(a). The first two bands cross each other at the diabolic points; hence there is no complete band gap between these bands,

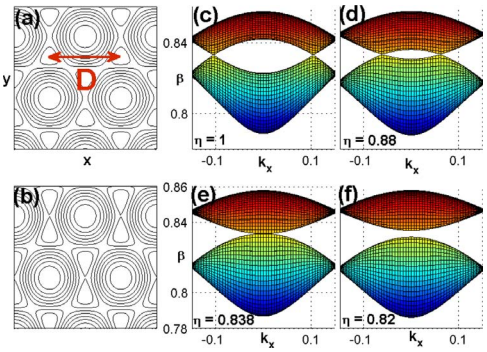

Fig. 1. (Color online) (a), (b) Lattice in real space for uniaxial deformation with $\eta=1,0.82$, respectively. (c)–(f) Side view of the band structure manifold of the propagation constant, β, for uniaxial deformation with $\eta=1,0.88,0.838,0.82$, respectively.

as shown in Fig. 1(c). Since the honeycomb lattice is not a Bravais lattice, in order to span it, one should include a basis vector in addition to the two primitive vectors. When $\eta_i < 1$ (reducing the amplitude of the ith wave, with $i=2,3$), the primitive lattice vectors and the unit cell remain unchanged. When $\eta_2 = \eta_3$ (uniaxial deformation), the only lattice parameter that has been modified is the basis vector separating the two sites inside the unit cell (in the tight binding picture). However, when $\eta_2 \neq \eta_3$ (biaxial deformation), the sites inside the unit cell are modified as well, forming a deformed honeycomb lattice with different atoms inside a unit cell.

We find that even an infinitesimal deviation of η from unity reduces the symmetry of the lattice. However, for uniaxial deformation, the degeneracy at the diabolic points is not removed, and the bands still cross each other even for significant deformations. As the deformation is increased, the diabolic points move toward each other, until η reaches a critical value $\eta_c \simeq 0.838$ where each pair of diabolic points merges, and a gap appears between the first two bands, shown in Figs. 1(c)–1(f). After the gap appears, the band is parabolic; hence excitations can no longer be treated as massless Dirac fermions. Note that η_c is not a universal value but depends on the lattice constant D and the potential details. For biaxial deformations, even extremely small, degeneracy is removed because the reflection symmetries (σ_x, σ_y) are broken; hence the bands no longer cross each other, and a tiny gap always opens up. However, in spite of the gap, we find that the vicinity of the extrema points still includes a large region where the dispersion curve is linear. Hence, many of the interesting features of the honeycomb lattice (chiral excitations, diffractionless region) remain even in a considerably deformed lattice, since their origin is not the diabolic points themselves, but their vicinity.

Next we study the linear propagation of a narrow beam centered at one of the diabolic points in a lattice with uniaxial deformation. We find that the cross section of each diabolic cone is no longer circular but elliptical. The gradient (in k space) of the propagation constant is the transverse velocity of each mode. For a circular cone, the velocity is isotropic; hence all the Bloch modes comprising the beam propagate at the same velocity, forming a ring [6]. When the honeycomb symmetry is slightly broken ($\eta \neq 1$ but still close to 1) in a uniaxial fashion, the cross section is elliptical; thus transverse velocity is no longer isotropic. An immediate consequence is that the beam broadens in one direction faster than in the other, yielding elliptical rings separated by a dark ring (similar to the dark rings observed in biaxial crystals [9]). The example in Fig. 2 displays a simulation of the linear version of Eq. (1) ($B=0$). We use dimensionless units, providing $n_0=2.3$ and $\Delta n_0 = 5\times 10^{-3}$, the propagation distance is 1.2 cm, and the radius of the rings is 150 μm. Figure 2(d) highlights the dependence of the axes ratio $R \equiv b/a$ (a, b are the axes of the ellipse) of the elliptical rings versus the deformation of the lattice for a uniaxial deformation. When the deformation is biaxial, the equi-surfaces

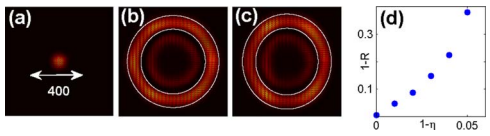

Fig. 2. (Color online) (a) Input beam with no angular dependence. (b) Conical diffraction; the equation of the contour is $(x/320)^2+(y/320)^2=1$. (c) Elliptical diffraction for $\eta=0.98$; the equation of the contour is $(x/310)^2+(y/330)^2=1$. (d) $1-R$ (R axes ratio) of the ellipses increases rapidly with deformation of the lattice.

around the extrema are oval; hence a narrow beam centered at the extremum point propagates into distorted elliptical rings with nonuniform intensity.

We proceed to study nonlinear waves in honeycomb photonic lattices. Reference [6] has demonstrated solitons in honeycomb lattices, residing in the gap between the second and third bands, but no solitons were found between the first and second bands. In this context, there is a common conjecture that (the propagation constant of) solitons in continuous periodic systems must reside in gaps (either the semi-infinite gap beyond the first band or the gap between two bands). An ideal honeycomb lattice has no complete band gap between the first two bands; hence it is expected that it would not support solitons arising from the edge of the first Brillouin zone. A honeycomb lattice with deformation beyond η_c does exhibit such a gap. Indeed, we find solitons in our deformed honeycomb lattices for any $\eta < 0.82$. The lattice can support a soliton only if the propagation constant of the soliton, β_s, resides inside the gap. We find solitons with typical intensities $B \sim 0.01-0.05$, much smaller than both 1 and I_{ind}; hence $\Delta n \simeq \Delta n_0/(1+I_{\mathrm{ind}}) - B\Delta n_0 |\psi^2|/(1+I_{\mathrm{ind}})^2 \equiv V_0 + BW$, where V_0 and W are linear and nonlinear contributions to Δn, respectively. Now we can express β_s in terms of B and $|\psi|^2$ and give an estimate for the gap. We find that $\beta_s = k/n_0(\langle\psi_s|H_0|\psi_s\rangle - B\langle\psi_s|W|\psi_s\rangle)$, where $H_0 = \nabla_\perp^2/(2k) + V_0 k/n_0$. Note that the soliton intensity has a maximal value, $B_{\max}$, since greater values push the soliton outside the gap into the second band (where it disintegrates); hence $\beta_{\max}^{(II)} \simeq \beta_s(B=B_{\max})$ (maximum of the second band). On the other hand, for vanishing B, $\beta_s(B=0) \simeq k/n_0\langle\psi_s|H_0|\psi_s\rangle$ coincides with $\beta_{\min}^{(I)}$ (minimum of the second band), and therefore the band gap is $\delta\beta \equiv |\beta_{\min}^{(I)} - \beta_{\max}^{(II)}| \approx B_{\min}\langle\psi_s|W|\psi_s\rangle$. One can therefore find the soliton existence range from experiments and calculate $\delta\beta$.

We follow the dynamics of a soliton as the lattice deformation is gradually decreased. We find that the localized nonlinear eigenstate of the system is a suitable probe for the existence of a given gap. Technically, we use the self-consistency method for a lattice with a specific deformation, find such an eigenstate, and study its dynamics by simulating its propagation using Eq. (1) for a variety of lattices in which the input is not an eigenstate, as shown in Fig. 3. Our simulations reveal that the dynamics of the nonlinear probe dramatically changes when the deformation crosses a threshold value (which depends on the intensity of the probe), for which the propagation

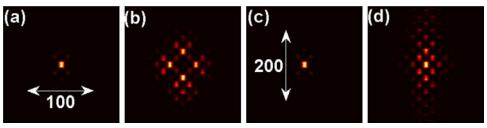

Fig. 3. (Color online) (a) Input intensity, (b) linear propagation of a nonlinear eigenstate at three diffraction lengths, (c) nonlinear propagation of a nonlinear eigenstate at ~30 diffraction lengths, and (d) nonlinear propagation in a lattice with a gap not large enough to support a gap soliton at three diffraction lengths.

constant (eigenvalue) β_s is too close to one of the bands.

The following describes our simulations where we launch such a localized beam into the deformed lattice, under various conditions. When the beam is propagating linearly in the slightly deformed (or nondeformed) lattice, it exhibits diffraction broadening after some propagation distance $Z_0 = 0.6$ cm, shown in Fig. 3(b). As we apply the nonlinearity, the behavior of the wavefunction dramatically changes for two cases. When the deformation is such that the gap is sufficiently large, the beam propagates without any significant change, as the input wavefunction adjusts adiabatically to the parameters of the deformed lattice. The actual value of the deformation ratio hardly affects the propagating wavefunction, and the probe beam evolves into a gap soliton, a stable nonlinear self-localized state, as shown in Fig. 3(c). This is true also when the probe beam is initially not an eigenstate of the lattice; the beam evolves into a gap soliton, as long as the lattice deformation is sufficient. However, as the lattice deformation decreases and crosses the threshold value, the gap is too small to support the particular nonlinear probe, and the wavepacket disintegrates, as shown in Fig. 3(d).

In conclusion, we have studied linear and nonlinear wave dynamics in deformed honeycomb lattices. As the lattice deformation increases, the diabolic points get closer together until they merge, then completely disappear, and a gap opens up between the first two bands. As the lattice increasingly deforms, conical diffraction of beams associated with the diabolic points becomes elliptic with its eccentricity rising rapidly with lattice deformation, accompanied by a dark ring. Once the lattice is sufficiently deformed, it can support a robust gap soliton residing in the gap between the first two bands. The existence of such a gap soliton can be used as an experimental probe for the presence of the gap, which provides an estimate of its magnitude. Last but not least, this work is in fact a precursor for exploring the intriguing possibility of observing Anderson localization in honeycomb lattices containing disorder. The technique to carry out such experiments was demonstrated recently [14]. However, investigating Anderson localization specifically in honeycomb lattices is so interesting exactly because of these diabolic points, with the unique transport properties of the Bloch modes associated with their vicinity. The present work shows unequivocally that, even when the degeneracy at the diabolic points is removed and very small gaps open up, the dispersion curve at the vicinity of these points is still linear, that is, dispersionless, even in the presence of considerable deformations of the honeycomb lattice. This is a crucial issue, because, if every small deformation had caused major modification of this unique dispersion curve, then the questions regarding localization on honeycomb lattices would simply reduce to known results in any 2D lattice. In this sense, the present work suggests that Anderson localization in honeycomb lattices will indeed exhibit unique features, arising from the unique transport properties at the vicinity of the diabolic points.

This work was supported by the Israel science Foundation and USA–Israel Binational Science Foundation.

References

1. P. R. Wallace, Nucl. Phys. Rev. **71**, 622 (1947).
2. K. S. Novoselov, A. K. Geim, S. V. Morozov, D. Jiang, M. I. Katsnelson, I. V. Grigorieva, S. V. Dubonos, and A. A. Firsov, Nature **197**, 438 (2005).
3. M. I. Katsnelson, Eur. Phys. J. B **51**, 157 (2006).
4. K. S. Novoselov, Z. Jiang, Y. Zhang, S. V. Morozov, H. L. Stormer, U. Zeitler, J. C. Maan, G. S. Boebinger, P. Kim, and A. K. Geim, Science **315**, 1379 (2007).
5. S.-L. Zhu, B. Wang, and L. M. Duan, Phys. Rev. Lett. **98**, 260402 (2007).
6. O. Peleg, G. Bartal, B. Freedman, O. Manela, M. Segev, and D. N. Christodoulides, Phys. Rev. Lett. **98**, 103901 (2007).
7. W. Hamilton, Trans. Roy. Irish Acad. **17**, 293 (1837).
8. H. Lloyd, Trans. Royal. Irish. Acad. **17**, 1 (1837).
9. M. Berry and M. Jeffrey, in *Progress in Optics*, E. Wolf, ed. (Elsevier, 2007), Vol. 50, pp. 13–50.
10. N. K. Efremidis, S. Sears, D. N. Christodoulides, J. W. Fleischer, and M. Segev, Phys. Rev. E **66**, 046602 (2002).
11. J. W. Fleischer, T. Carmon, M. Segev, N. K. Efremidis, and D. N. Christodoulides, Phys. Rev. Lett. **90**, 023902 (2003).
12. J. W. Fleischer, M. Segev, N. K. Efremidis, and D. N. Christodoulides, Nature **422**, 147 (2007).
13. M. Segev, G. C. Valley, B. Crosignani, P. DiPorto, and A. Yariv, Phys. Rev. Lett. **73**, 3211 (1994).
14. T. Schwartz, G. Bartal, S. Fishman, and M. Segev, Nature **446**, 52 (2007).